JSHC
Japan Society of
Histochemistry and Cytochemistry
Established 1959

Acta Histochem. Cytochem. 56 (6): 111–119, 2023
doi: 10.1267/ahc.23-00041

Regular Article

Cyclin D3 Colocalizes with Myogenin and p21 in Skeletal Muscle Satellite Cells during Early-Stage Functional Overload

Minenori Ishido

Section for Health-related Physical Education, Division of Human Sciences, Faculty of Engineering, Osaka Institute of Technology, Osaka 535–8585, Japan

Received June 2, 2023; accepted October 9, 2023; published online December 20, 2023

Myogenic cell differentiation is modulated by multiple regulatory factors, such as myogenin, p21, and cyclin D3 during myogenesis *in vitro*. It is also recognized that myogenin and p21 play important roles in regulating muscle satellite cell (SC) differentiation during overload-induced muscle hypertrophy *in vivo*. However, the expression patterns and functional role of cyclin D3 in the progress of muscle hypertrophy remain unclear. Thus, the present study investigated cyclin D3 expression in skeletal muscles during early-stage functional overload. Plantaris muscles were exposed to functional overload due to ablation of the gastrocnemius and soleus muscles. As a result, cyclin D3 expression was detected in the nuclei of SCs but not in myonuclei on day 1 after surgery. Cyclin D3 expression, after functional overload, gradually increased, reaching a maximum on day 7 along with myogenin expression. Moreover, in response to the functional overload, cyclin D3 was expressed simultaneously with myogenin and p21 in SC nuclei. Therefore, the present study suggests that cyclin D3 with myogenin and p21 may interactively regulate SC differentiation during early-stage functional overload.

Key words: skeletal muscle, cyclin D3, muscle hypertrophy, satellite cell

I. Introduction

Skeletal muscles induce muscle hypertrophy in response to increased muscle activities like functional overload. Among muscle hypertrophy-related processes, those involving muscle SCs, such as activation, proliferation, differentiation, and fusion to existing myofibers, are essential [12, 31]. SC differentiation is particularly essential for muscle hypertrophy processes prior to SC fusion with existing myofibers.

During myogenesis, the differentiation of myogenic cells, like SCs, is interactively modulated by multiple regulatory factors *in vitro*, including myogenin, p21, retinoblastoma tumor suppressor protein, and cyclin D3 [1, 2, 6, 8, 34, 39]. Cyclin D3 is a particularly interesting factor for myogenic cell differentiation.

Cyclin D3 is of the cyclin D family (cyclin D1, etc.). This family, represented by cyclin D1, is pivotal in cell cycle promotion and inhibiting differentiation [29, 32]. Cyclin D3 is an exception, however, shown to be deeply involved in cell differentiation but not in the cell cycle [2]. In fact, during myogenesis, cyclin D3 is reported to regulate myogenic cell differentiation by inhibiting cyclin-dependent kinase 2 activity *in vitro* [4]. The previous study also demonstrated cyclin D3-mediated reorganization of internal Lamin, a major filament component underlying the nuclear lamina, and highlighted the critical role played in regulating myogenic cell differentiation [25]. Moreover, cyclin D3 deficiency both decreased the number of differentiated myocytes and resulted in immature differentiation states, thus reducing the number and size of myotubes formed *in vitro* [5]. Interestingly, a recent study reported that cyclin D3 may be involved in regulating myofiber type transition and skeletal muscle energy metabolism [9].

Correspondence to: Minenori Ishido, Division of Human Sciences, Osaka Institute of Technology, Ohmiya, Asahi-ku, Osaka 535–8585, Japan.
E-mail: minenori.ishido@oit.ac.jp

These findings show that cyclin D3 is a key regulatory factor in myogenic cell differentiation *in vitro*. However, during muscle hypertrophy *in vivo*, the expression patterns and functional role of cyclin D3 in SCs remain unclear. Therefore, the present study investigated the properties of cyclin D3 expression in skeletal muscle during early-stage functional overload.

II. Materials and Methods

Experimental design and surgical procedure

Eight-week-old female Fischer 344 rats were used in this study (n = 6/group). Between 2–3 rats were housed in each cage at 22°C with a 12 h light/dark cycle and were provided food and water *ad libitum*. All experiments were carried out following approval from the Ethics Committee on Life Sciences of Osaka Institute of Technology.

To produce overload-induced muscle hypertrophy, the plantaris muscle received ablation of the ipsilateral synergistic gastrocnemius and soleus muscles, as described previously [13, 18, 19]. Briefly, with the rats under pentobarbital sodium anesthesia (60 mg kg^{-1} i.p.) and inhalation anesthesia with 0.7% isoflurane, a skin incision was made to fully expose the dorsal region of the experimental leg. The soleus muscle was completely removed except for a small portion at the proximal end, where it attaches to the plantaris. Both the lateral and medial gastrocnemius muscles were completely removed. Contralateral plantaris muscles were used as sham-operated controls. At 1, 3, 5, and 7 days after surgery, the animals were sacrificed under pentobarbital sodium anesthesia (60 mg kg^{-1} i.p.) and inhalation anesthesia with 0.7% isoflurane. The plantaris muscles were removed and samples were frozen in liquid nitrogen and stored at −80°C until use.

Immunostaining

The primary antibodies used in the present study were as follows; rabbit polyclonal anti-laminin (a marker molecule for the basement membrane; 1:3000; Sigma, St Louis, MO), goat polyclonal anti-M-cadherin (a previously determined SC marker molecule [12, 18]) (1:200; Santa Cruz Biotech., Santa Cruz, CA), mouse monoclonal anti-cyclin D3, rabbit polyclonal anti-dystrophin (a marker molecule for the plasma membrane) (1:100; NeoMarkers, Fremont, CA, USA), rabbit polyclonal anti-myogenin (1:100; Santa Cruz Biotech.), mouse monoclonal anti-myogenin (1:100; BD PharMingen, San Diego, CA, USA), rabbit polyclonal anti-cyclin-dependent kinase inhibitor p21 (Ab-5, 1:100; Oncogen Research Products, Cambridge, MA, USA) and rabbit polyclonal anti-Ki67 (1:100; Novocastra, Newcastle upon Tyne, UK). Ki67 was used as the marker molecular for proliferating SCs [10, 30]. Myogenin and p21 were used as marker molecules for differentiating SCs [11, 20, 33, 40].

For immunostaining, serial cross-sections (5 or 10 μm thickness) of mid-belly muscles were cut using a cryostat at −20°C and thawed on 3-amino propylethoxysilane-coated slides. The sections were fixed with 4% paraformaldehyde in 0.1 M phosphate buffer (pH 7.4) for 15 min and washed with 0.1 M phosphate-buffered saline (PBS, pH 7.4). To block non-specific reactions, the sections were incubated with 0.1 M PBS containing 10% normal serum and 1% Triton X-100 for 1 h. The primary antibodies were diluted as required with 0.1 M PBS containing 5% normal serum and 0.3% Triton X-100, and the secondary antibodies were diluted as required with 0.1 M PBS containing 5% normal serum and 0.1% Triton X-100.

For triple fluorescence staining, the sections were simultaneously incubated for 16 h to 48 h at 4°C with the primary antibodies. They were washed in 0.1 M PBS and simultaneously incubated overnight at 4°C with secondary antibodies. The secondary antibodies used in this study were fluorescein-labeled horse anti-mouse IgG (1:300; Vector Labs), rhodamine-labeled goat anti-rabbit IgG (1:300; Chemicon, Temecala, CA) or Alexa Fluor 568-labeled donkey anti-goat IgG (1:300; Molecular Probes, Eugene, OR). The sections were washed in 0.1 M PBS and mounted in Vectashield mounting medium with DAPI (Vector Labs) to visualize the nuclei. Image analysis was performed with the fluorescence microscope (Bx51, Olympus Co., Tokyo, Japan) and RS image (Roper Scientific Inc., Chiba, Japan).

Quantitative analysis

Myofiber quantitative analysis showing positive immunoreactivities in SCs was performed using a method described elsewhere [7, 18, 38]. All myofibers in a cross-section were analyzed for each sample. Myofibers showing cyclin D3-, myogenin-positive immunoreactivities in the nuclei of M-cadherin-positive SCs were counted on days 1, 3, 5, and 7 post-surgery and are presented as a percentage of the total myofiber number counted in the same cross-section.

Statistical analysis

All data are presented as the mean ± SD and were analyzed with StatView (SAS institute Inc., Cary, NC). Differences in relative muscle weight between the overloaded muscles and post-surgery-matched contralateral sham-operated muscles were tested by paired t-test. Differences among the groups in which the expression of cyclin D3 and myogenin (days 1, 3, 5, and 7 post-surgery) was detected in the nuclei of SCs were tested by one-way ANOVA using Scheffé's S test. It should be noted that differences between the overloaded muscles and contralateral sham-operated control muscles were not tested, as the expression of cyclin D3 and myogenin was not detected in the nuclei of SCs in the sham-operated controls. Differences were considered significant at the $p < 0.05$ confidence level.

III. Results

The relative weights of the plantaris muscles over-

Table 1. *Time course changes in relative muscle weight in contralateral sham-operated and overloaded plantaris muscles*

Time post-surgery (days)	group	
	CS	OV
1	94.11 ± 8.34	142.21 ± 5.35*
3	94.84 ± 7.38	138.80 ± 14.62*
5	90.52 ± 3.26	122.81 ± 9.07*
7	94.53 ± 7.50	121.18 ± 9.34*

Values are mean ± SD.
Relative muscle weight is presented as a mg per 100 g body weight.
CS: contralateral sham-operated muscles. OV: overloaded muscles.
* Significant difference from post-surgery-matched contralateral sham-operated muscles ($p < 0.05$).

loaded by synergistic ablation were significantly increased compared with the contralateral sham-operated muscles throughout the experimental periods ($p < 0.05$) (Table 1). These results indicate the surgical procedure was sufficient to induce compensatory hypertrophy in the functionally overloaded skeletal muscles.

Localization and expression patterns of cyclin D3 in overloaded skeletal muscle

To confirm whether cyclin D3 expression was induced in the plantaris muscles during early-stage functional overload, immunostaining was performed on post-surgery day 1 using anti-cyclin D3 and DAPI. This identified cyclin D3-positive immunoreactivities in DAPI-positive nuclei (Fig. 1a–c). Furthermore, cyclin D3 positive-immunoreactivities were detected in nuclei located inside laminin-positive basement membranes (Fig. 1d–g). These findings indicated that cyclin D3 expression was induced in the nuclei associated with myofibers during early-stage functional overload.

To identify whether cyclin D3 expression was induced in myonuclei during early-stage functional overload, immunostaining was performed with anti-cyclin D3, anti-dystrophin, and DAPI on post-surgery day 1 (Fig. 2a–d). This detected no cyclin D3-positive immunoreactivity in nuclei located inside dystrophin-positive plasma membranes. On the other hand, immunostaining with anti-cyclin D3, anti-M-cadherin, and DAPI was performed on post-surgery day 1 (Fig. 2e–h). M-caherin is one of the membrane proteins that specifically localize to the plasma membrane of muscle satellite cells and is widely recognized as a molecular marker for muscle satellite cells [12, 18]. Cyclin D3-positive immunoreactivities were detected in the nuclei of M-cadherin-positive SCs. These findings indicate that cyclin D3 is expressed in the nuclei of SCs, but not in myonuclei during early-stage functional overload.

In addition, the cyclin D3 time course changes were examined in the SC nuclei of overloaded muscles (Fig. 3). The percentage of myofibers with cyclin D3-positive

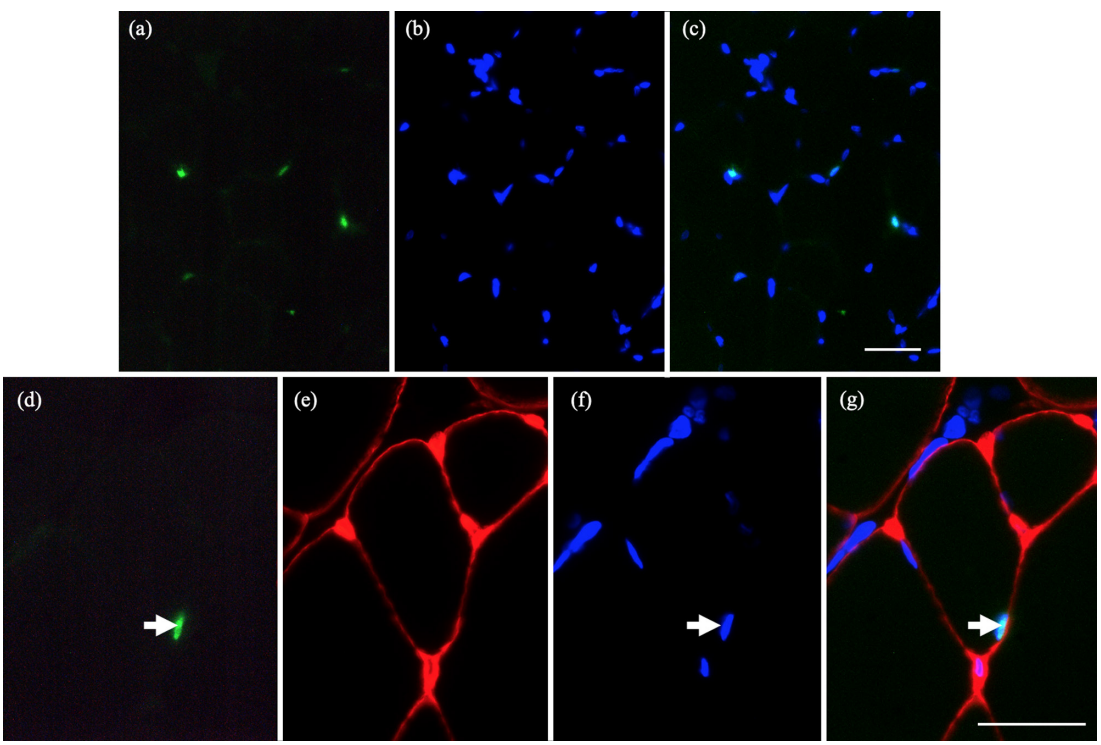

Fig. 1. Photomicrographs showing cyclin D3 localization in post-surgery day 1 overloaded muscles. Immunostaining was performed to visualize the localization of cyclin D3 (**a**) and nuclei (**b**), and the two merged images (**c**). Immunostaining was performed to visualize the localization of cyclin D3 (**d**), laminin (**e**), and nuclei (**f**), and the three merged images (**g**). The arrows in (**d**), (**f**), and (**g**) indicate cyclin D3-positive nuclei located inside the laminin-positive basement membrane of myofibers. Bar = 30 μm.

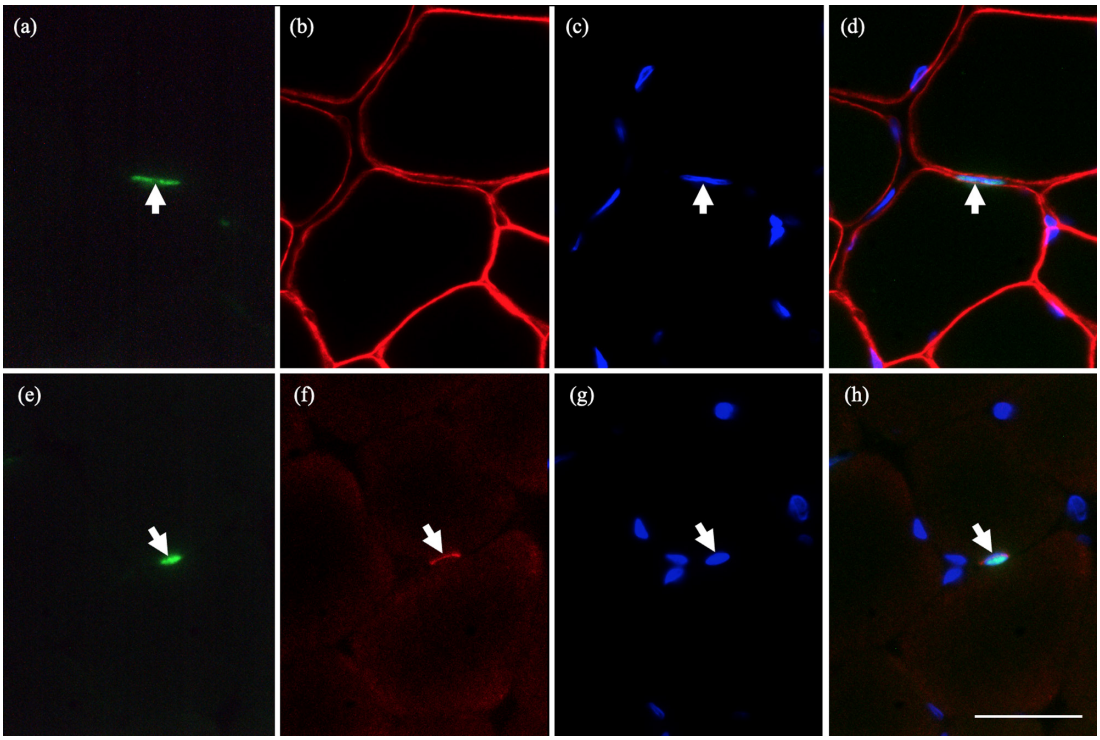

Fig. 2. Photomicrographs of overloaded muscles on post-surgery day 1 showing the expression of cyclin D3 in the nuclei of satellite cells (SCs) but not myonuclei. Immunostaining was performed to visualize the localization of cyclin D3 (**a**), dystrophin (**b**), and nuclei (**c**), and the three images merged (**d**). The arrows in (**a**), (**c**), and (**d**) indicate cyclin D3-positive nuclei located outside the dystrophin-positive plasma membrane of myofibers. Immunostaining was performed to visualize the localization of cyclin D3 (**e**), M-cadherin (**f**), nuclei (**g**), and the three images merged (**h**). The arrows in (**e**), (**g**), and (**h**) indicate cyclin D3-positive nuclei expressed in an M-cadherin-positive SC. Bar = 30 μm.

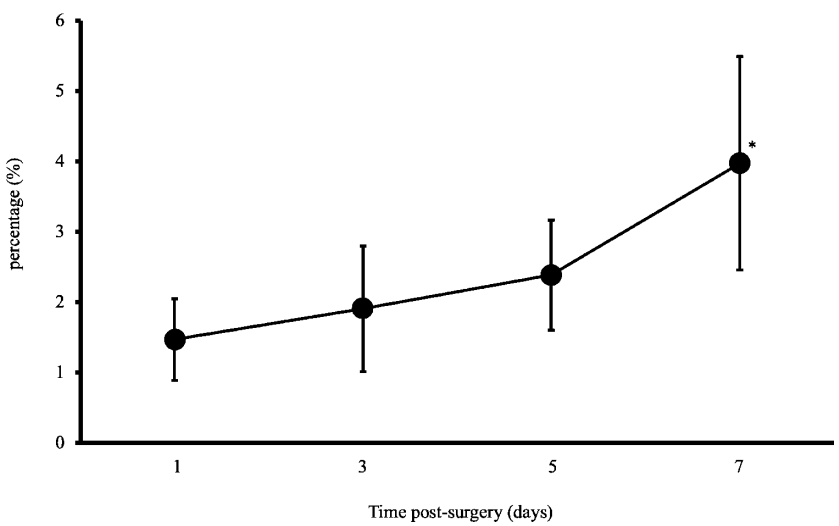

Fig. 3. The expression patterns of cyclin D3 in satellite cell (SC) nuclei of overloaded muscles. The line graph indicates time course changes in the percentage of myofibers with SC nuclei expressing cyclin D3. Values are the mean ± SD. Note: in the contralateral sham-operated muscles, neither cyclin D3 nor myogenin expression was detected in the nuclei of SCs throughout the experimental periods. * Significantly different compared with post-surgery day 1 and 3 muscles ($p < 0.05$).

immunoreactivities in the nuclei of M-cadherin-positive SCs significantly increased by post-surgery day 7, compared with day 1 and 3 post-surgery ($p < 0.05$, respectively). Moreover, although no significant difference was detected between day 5 and 7 post-surgery, the percentage of cyclin D3 expression in SCs on post-surgery day 7 was slightly larger than on day 5. These findings indicate that cyclin D3 expression in SCs increases over time during early-stage functional overload.

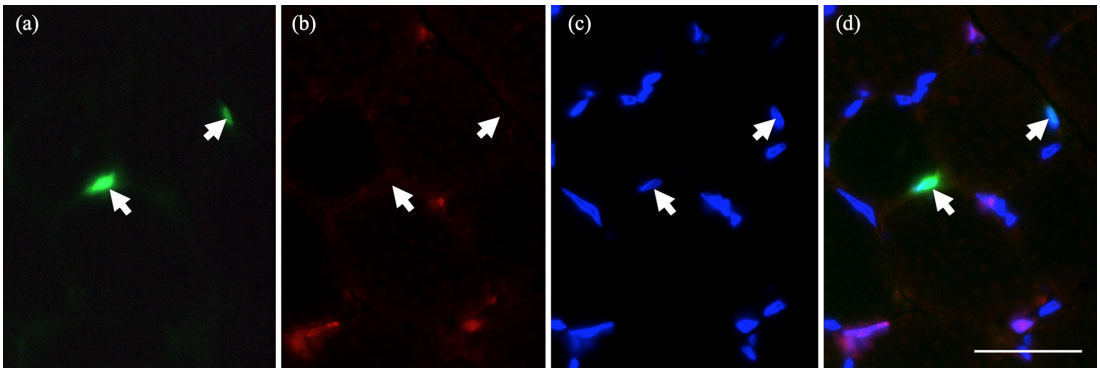

Fig. 4. Photomicrographs of post-surgery day 1 overloaded muscles showing the relationship between cyclin D3 and Ki67 in a satellite cell (SC) nucleus. Immunostaining was performed to visualize the localization of cyclin D3 (**a**), Ki67 (**b**), nuclei (**c**), and the three images merged (**d**). The arrows in (**a**)–(**d**) indicate a DAPI-positive nucleus expressing cyclin D3 but not Ki67. Bar = 30 μm.

The expression of cyclin D3 on the nuclei of proliferating SCs during early-stage functional overload

To elucidate the role of cyclin D3 expressed in SC nuclei during early-stage functional overload, immunostaining was performed with anti-cyclin D3, anti-Ki67, and DAPI on post-surgery day 1 (Fig. 4a–d). This identified no colocalization in any nuclei of cyclin D3 and Ki67. These findings show that cyclin D3 expression was not induced in the nuclei of proliferating SCs during early-stage functional overload.

The relationship among cyclin D3, myogenin, and p21 expression on the nuclei of differentiating SCs during early-stage functional overload

Immunostaining was performed on post-surgery day 7 with anti-myogenin, anti-M-cadherin, and DAPI, detecting myogenin-positive immunoreactivities in the nuclei of M-cadherin-positive SCs (Fig. 5a–d). In addition, on post-surgery day 7 there was a significant increase in the percentage of myofibers with myogenin-positive immunoreactivities in the nuclei of M-cadherin-positive SCs, compared with post-surgery days 1, 3, and 5 ($p < 0.05$, respectively) (Fig. 5e). These findings indicated that myogenin expression in SCs increases over time during early-stage functional overload, as well as cyclin D3 expression.

The relationship between cyclin D3 and myogenin during early-stage functional overload was then examined. After immunostaining on post-surgery day 7, with anti-cyclin D3, anti-myogenin, and DAPI, the colocalization of cyclin D3 and myogenin was detected in the nuclei of SCs (Fig. 6a–d). Furthermore, after immunostaining with anti-cyclin D3, anti-p21, and DAPI, the colocalization of cyclin D3 and p21 was also detected in the nuclei of SCs on post-surgery day 7 (Fig. 6e–h). Finally, the colocalization of myogenin and p21 was detected in the nuclei of SCs on post-surgery day 7 (Fig. 6i–l) after immunostaining with anti-myogenin, anti-p21, and DAPI.

Next, the colocalization of cyclin D3, myogenin, and p21 was examined in differentiated SCs during early-stage functional overload. The SC nucleus length in rats is approximately 9–12 μm [37] and if 5 μm serial sections are cut, the SC nucleus can be divided twice. Therefore, 5 μm serial sections were prepared according to previous studies [16, 17]. First, to detect the colocalization of cyclin D3 and myogenin in the differentiated SCs of muscles on post-surgery day 5, a serial section was immunostained for cyclin D3, myogenin, and with DAPI, then the section adjacent was immunostained for cyclin D3, p21, and with DAPI (Fig. 7, A-d). Myogenin and p21 were colocalized in an SC expressing cyclin D3 in its nucleus. These results demonstrate cyclin D3 colocalization with myogenin and p21 in SCs differentiation stages during early-stage functional overload.

IV. Discussion

The increases in relative muscle weight in plantaris muscles shown in the present study were consistent with previous studies that investigated plantaris muscle hypertrophy during early-stage functional overload [14, 18, 28]. Therefore, in the present study, functional overload was confirmed to induce muscle hypertrophy from an early stage.

In general, the myonuclei have lost mitosis capacity in the skeletal muscle *in vivo* [27, 35]. Therefore, as D-type cyclins, including cyclin D3, are fundamental regulatory factors of proliferation/differentiation processes [3, 32], the present study's detection of cyclin D3 expression in SCs but not myonuclei is reasonable.

In the current study, the expression of cyclin D3 were not colocalized with that of Ki67 in the nucleus in functional overloaded skeletal muscles throughout the experimental periods. These results were supported by the previous studies which demonstrated that cyclin D3 fundamentally regulates the cell differentiation of cells, but not cell proliferation, by interacting with retinoblastoma, which is key factor to regulate the cell differentiation [2, 6, 23]. On the other hand, the current study could not identify the cell type of Ki67-expressing cells. Hence, it was not ruled out the possibility that Ki67 was expressing in cells other

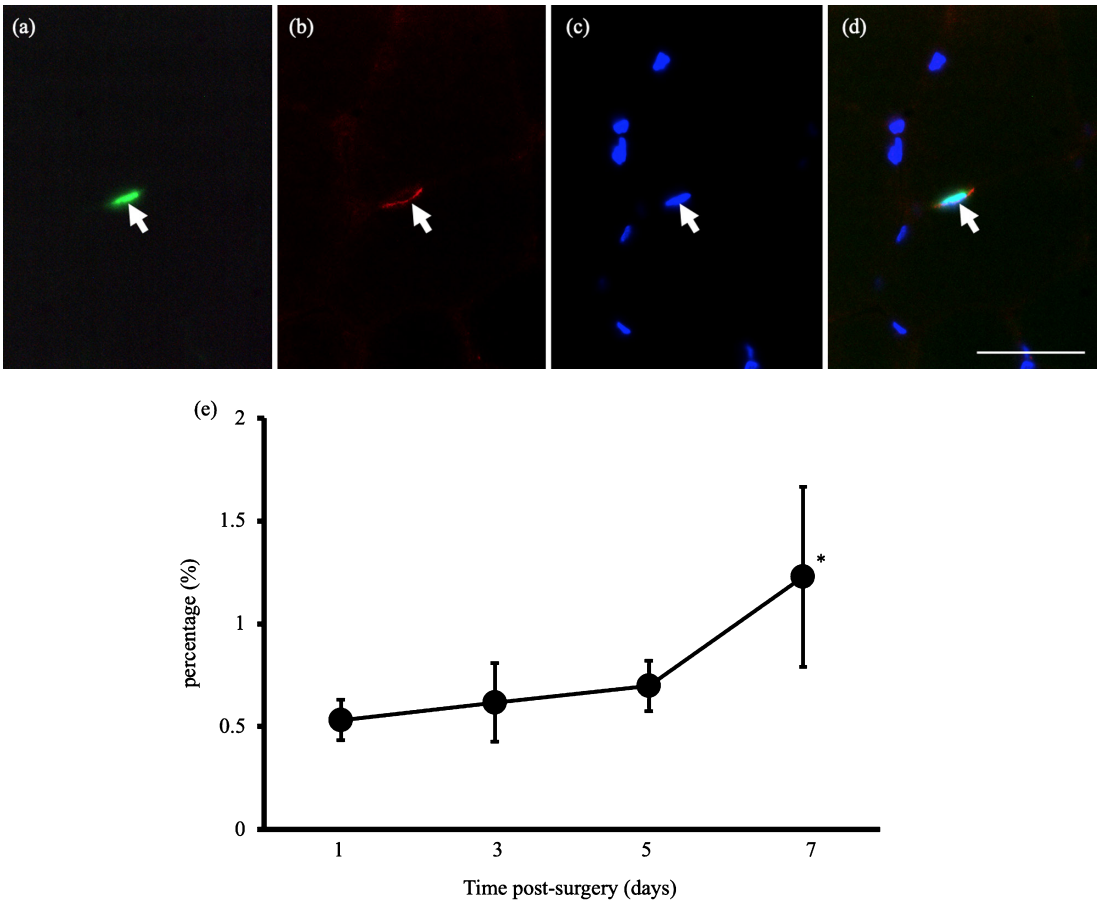

Fig. 5. The expression patterns of myogenin in satellite cell (SC) nuclei in overloaded muscles. In post-surgery day 7 overloaded muscles, immunostaining was performed to visualize the localization of myogenin (**a**), M-cadherin (**b**), nuclei (**c**), and the three merged images (**d**). The arrows in (**a**), (**c**), and (**d**) indicate myogenin-positive nuclei expressed in an M-cadherin-positive SC. Bar = 30 µm. (**e**) time course changes in the percentage of myofibers with SC nuclei expressing myogenin in overloaded muscles. Values are the mean ± SD. Note: in the contralateral sham-operated muscles, neither myogenin nor myogenin expression was detected in the nuclei of SCs throughout the experimental periods. *Significantly different compared with post-surgery days 1, 3, and 5 in overloaded muscles ($p < 0.05$).

than muscle satellite cells. For example, the previous studies indicated that in addition to the muscle satellite cells muscle-derived stem cells located in the interstitial spaces between myofibers were activated in the skeletal muscles during muscle development such as muscle hypertrophy [16, 36]. Therefore, in the current study, Ki67-expressing cells may possibly be the activated muscle-derived stem cells in addition to the muscles satellite cells. Moreover, the previous studies demonstrated that the remodeling of extracellular matrix was induced by the increase of skeletal muscle activities [22, 26, 42]. Therefore, it was not ruled out the possibility that the fibroblasts located in the interstitial spaces between myofibers were activated in response to the increase of muscle activities during the functional overload in the current study. In addition, the current study could not exclude the possibility that not all cells in proliferative phase had been detected due to technical limitations of immunohistochemical staining. Thus, further studies are needed to conclude on the involvement of cyclinD3 in the proliferation phase of muscle satellite cells.

After functional overload, the rate of SCs expressing cyclin D3 gradually increased, and reached a maximum on day 7. The expression pattern changes of cyclin D3 in the SC functional overload response were similar to myogenin in SCs during early-stage functional overload indicated by the present and previous studies [15, 18]. In fact, the colocalization of cyclin D3 and myogenin was detected in the SC nuclei of overloaded muscles. Moreover, the colocalization of cyclin D3, myogenin, and p21 was detected in the nucleus of SCs in the overloaded muscles. It is well-known that myogenin and p21 are key factors in regulating myogenic cell differentiation [1, 24, 33, 41]. For example, studies demonstrated the important roles myogenin and p21 play in regulating SC differentiation during muscle regeneration and hypertrophy *in vivo* [15, 21]. Although, previous studies reported cyclin D3 participation in regulating differentiation but not the proliferation of myogenic cells *in vitro* [2–4]. The functional roles of cyclin D3 in morphological changes of skeletal muscle involving muscle SC differentiation, such as regeneration and hypertrophy, remain

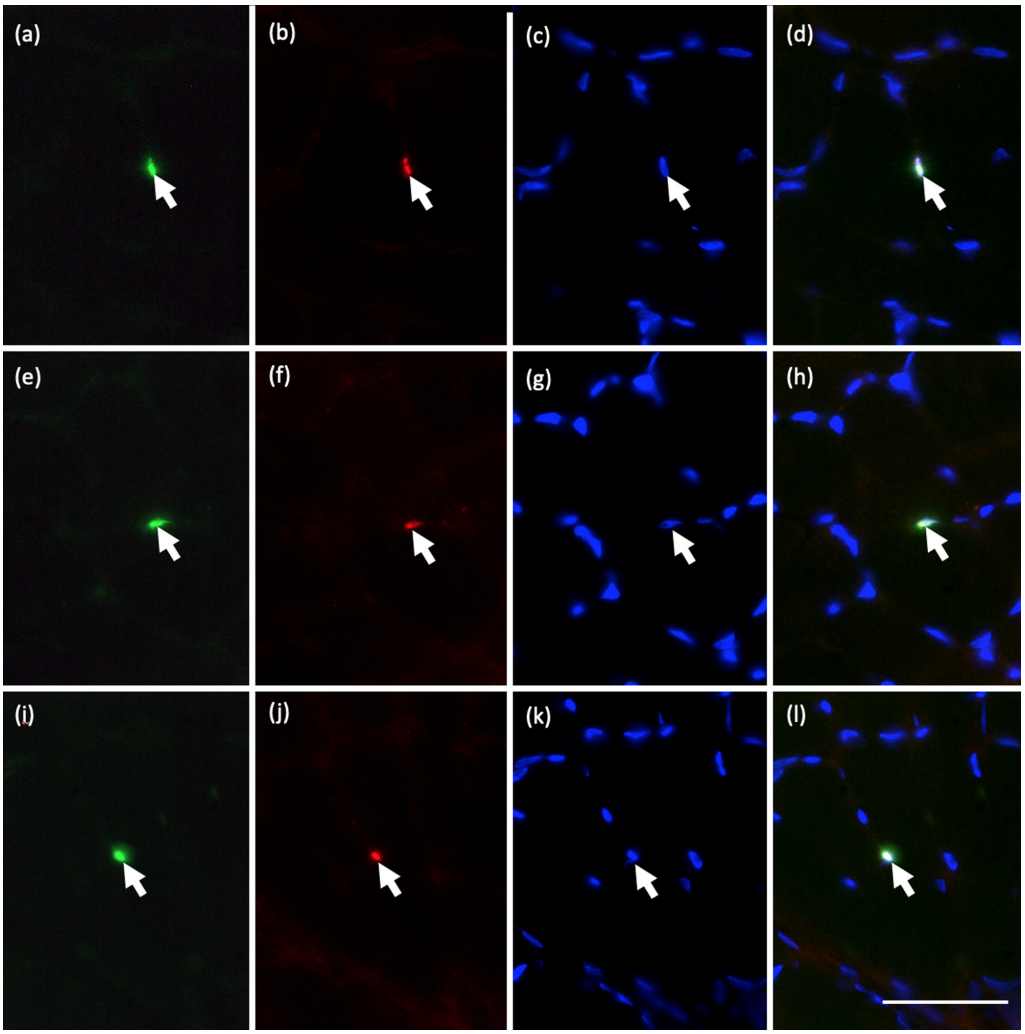

Fig. 6. Photomicrographs of post-surgery day 7 overloaded muscles showing the relationship between myogenin and p21 in a satellite cell (SC) nucleus. Immunostaining was performed to visualize the localization of cyclin D3 (**a**), myogenin (**b**), and nuclei (**c**), and the three images merged (**d**). The arrows in (**a**)–(**d**) indicate the coexpression of cyclin and myogenin in an SC. Immunostaining was performed to visualize the localization of cyclin D3 (**e**), p21 (**f**), and nuclei (**g**), and the three images merged (**h**). The arrows in (**e**)–(**h**) indicate myogenin and p21 coexpression in an SC. Immunostaining was performed to visualize the localization of myogenin (**i**), p21 (**j**), and nuclei (**k**), and the three images merged (**l**). The arrows in (**i**)–(**l**) indicate myogenin and p21 coexpression in a SC. Bar = 30 μm.

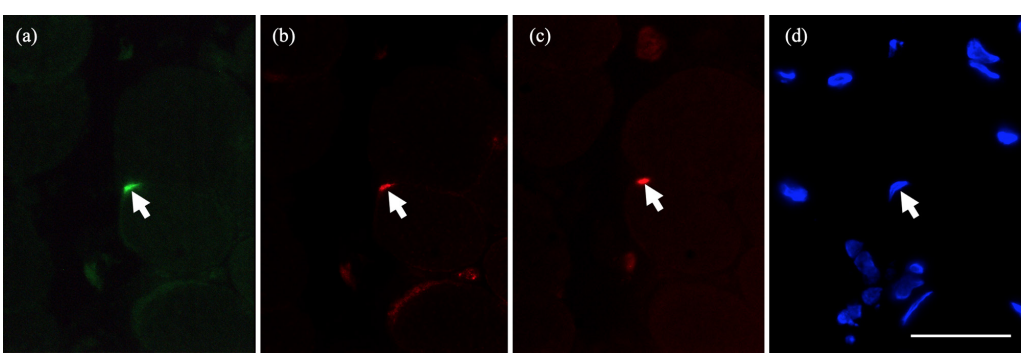

Fig. 7. Photomicrographs of post-surgery day 5 overloaded muscles showing the coexpression of cyclin D3, myogenin, and p21. Triple fluorescence staining to visualize the localization of cyclin D3 (**a**), myogenin (**b**), p21 (**c**), and nuclei (**d**) were performed. An adjacent serial section of post-surgery day 5 overloaded muscle was prepared at 5 μm thickness and immunostained for cyclin D3/myogenin/p21 and with DAPI. Arrows (**a**)–(**d**) indicate coexpression of cyclin D3, myogenin and p21-positive immunoreactivities in a nucleus. Bar = 30 μm.

unclear until now. The present study, for the first time, indicated the simultaneous expression of cyclin D3 with myogenin and p21 in differentiating SCs of overloaded skeletal muscle which suggests that cyclin D3 may jointly regulate, with myogenin and p21, the differentiation of SCs during early-stage functional overload.

In conclusion, the rate of SC cyclin D3 and myogenin expression gradually increased after functional overload, reaching the highest value on post-surgery day 7. Moreover, cyclin D3 was shown to colocalize with myogenin and p21 in the SC nucleus of overloaded skeletal muscles. Therefore, it is suggested that cyclin D3 may interactively regulate the differentiation of SCs with myogenin and p21 during early-stage functional overload.

V. Conflict of Interest

The author declare that no conflicts of interest exist.

VI. References

1. Andres, V. and Walsh, K. (1996) Myogenin expression, cell cycle withdrawal, and phenotypic differentiation are temporally separable events that precede cell fusion upon myogenesis. *J. Cell Biol.* 132; 657–666.
2. Bartkova, J. and Lukas, J. (1998) Cyclin D3: requirement for G1/S transition and high abundance in quiescent tissues suggest a dual role in proliferation and differentiation. *Oncogene.* 17; 1027–1037.
3. Cenciarelli, C. and De Santa, F. (1999) Critical role played by cyclin D3 in the MyoD-mediated arrest of cell cycle during myoblast differentiation. *Mol. Cell Biol.* 19; 5203–5217.
4. Chu, C. Y. and Lim, R. W. (2000) Involvement of p27(kip1) and cyclin D3 in the regulation of cdk2 activity during skeletal muscle differentiation. *Biochim. Biophys. Acta.* 1497; 175–185.
5. De Luca, G., Ferretti, R., Bruschi, M., Mezzaroma, E. and Caruso, M. (2013) Cyclin D3 critically regulates the balance between self-renewal and differentiation in skeletal muscle stem cells. *Stem. Cells* 31; 2478–2491.
6. De Santa, F., Albini, S., Mezzaroma, E., Baron, L., Felsani, A. and Caruso, M. (2007) pRb-dependent cyclin D3 protein stabilization is required for myogenic differentiation. *Mol. Cell Biol.* 27; 7248–7265.
7. Dedkov, E. I. and Borisov, A. B. (2003) Aging of skeletal muscle does not affect the response of satellite cells to denervation. *J. Histochem. Cytochem.* 51; 853–863.
8. Dhawan, J. and Rando, T. A. (2005) Stem cells in postnatal myogenesis: molecular mechanisms of satellite cell quiescence, activation and replenishment. *Trends. Cell Biol.* 15; 666–673.
9. Giannattasio, S., Giacovazzo, G., Bonato, A., Caruso, C., Luvisetto, S., Coccurello, R., *et al.* (2018) Lack of cyclin D3 induces skeletal muscle fiber-type shifting, increased endurance performance and hypermetabolism. *Sci. Rep.* 8; 12792.
10. Gorbe, A., Becker, D. L., Dux, L., Stelkovics, E., Krenacs, L., Bagdi, E., *et al.* (2005) Transient upregulation of connexin43 gap junctions and synchronized cell cycle control precede myoblast fusion in regenerating skeletal muscle in vivo. *Histochem. Cell Biol.* 123; 573–583.
11. Halevy, O. and Novitch, B. G. (1995) Correlation of terminal cell cycle arrest of skeletal muscle with induction of p21 by MyoD. *Science.* 267; 1018–1021.
12. Hawke, T. J. and Garry, D. J. (2001) Myogenic satellite cells: physiology to molecular biology. *J. Appl. Physiol.* 91; 534–551.
13. Ianuzzo, C. D. and Chen, V. (1977) Compensatory hypertrophy of skeletal muscle: contractile characteristics. *Physiol. Teach.* 6; 4–7.
14. Ianuzzo, C. D. (1979) Metabolic character of hypertrophied rat muscle. *J. Appl. Physiol.: Respirat. Environ. Exercise. Physiol.* 46; 738–742.
15. Ishido, M., Kami, K. and Masuhara, M. (2004) Localization of MyoD, myogenin and cell cycle regulatory factors in hypertrophying rat skeletal muscles. *Acta Physiol. Scand.* 180; 281–289.
16. Ishido, M., Kami, K. and Masuhara, M. (2004) In vivo expression patterns of MyoD, p21, and Rb proteins in myonuclei and satellite cells of denervated rat skeletal muscle. *Am. J. Physiol. Cell Physiol.* 287; C484–C493.
17. Ishido, M., Uda, M., Masuhara, M. and Kami, K. (2006) Alterations of M-cadherin, neural cell adhesion molecule and beta-catenin expression in satellite cells during overload-induced skeletal muscle hypertrophy. *Acta Physiol. (Oxf).* 187; 407–418.
18. Ishido, M., Uda, M., Kasuga, N. and Masuhara, M. (2009) The expression patterns of Pax7 in satellite cells during overload-induced rat adult skeletal muscle hypertrophy. *Acta Physiol. (Oxf).* 195; 459–469.
19. Ishido, M. and Nakamura, T. (2016) Aquaporin-4 Protein Is Stably Maintained in the Hypertrophied Muscles by Functional Overload. *Acta Histochem. Cytochem.* 49; 89–95.
20. Johnson, S. E. and Allen, R. E. (1993) Proliferating cell nuclear antigen (PCNA) is expressed in activated rat skeletal muscle satellite cells. *J. Cell Physiol.* 154; 39–43.
21. Kami, K. and Senba, E. (2002) In vivo activation of STAT3 signaling in satellite cells and myofibers in regenerating rat skeletal muscles. *J. Histochem. Cytochem.* 50; 1579–1589.
22. Kanazawa, Y., Nagano, M., Koinuma, S., Sugiyo, S. and Shigeyoshi, Y. (2021) Effects of Endurance Exercise on Basement Membrane in the Soleus Muscle of Aged Rats. *Acta Histochem. Cytochem.* 54; 167–175.
23. Kiess, M., Gill, R. M. and Hamel, P. A. (1995) Expression of the positive regulator of cell cycle progression, cyclin D3, is induced during differentiation of myoblasts into quiescent myotubes. *Oncogene.* 10; 159–166.
24. Mal, A. and Chattopadhyay, D. (2000) p21 and retinoblastoma protein control the absence of DNA replication in terminally differentiated muscle cells. *J. Cell Biol.* 149; 281–292.
25. Mariappan, I. and Parnaik, V. K. (2005) Sequestration of pRb by cyclin D3 causes intranuclear reorganization of lamin A/C during muscle cell differentiation. *Mol. Biol. Cell* 16; 1948–1960.
26. Mendias, C. L., Schwartz, A. J., Grekin, J. A., Gumucio, J. P. and Sugg, K. B. (2017) Changes in muscle fiber contractility and extracellular matrix production during skeletal muscle hypertrophy. *J. Appl. Physiol.* 122; 571–579.
27. Okazaki, K. and Holtzer, H. (1966) Myogenesis: Fusion, myosin synthesis, and the mitotic cycle. *Proc. Natl. Acad. Sci. U S A* 59; 1484–1490.
28. Plyley, M. J. and Olmstead, B. J. (1998) Time course of changes in capillarization in hypertrophied rat plantaris muscle. *J. Appl. Physiol.* 84; 902–907.
29. Rao, S. S. and Kohtz, D. S. (1995) Positive and negative regulation of D-type cyclin expression in skeletal myoblasts by basic fibroblast growth factor and transforming growth factor beta. A role for cyclin D1 in control of myoblast differentiation. *J. Biol. Chem.* 270; 4093–4100.
30. Reidy, P. T., Fry, C. S., Dickinson, J. M., Drummond, M. J. and Rasmussen, B. B. (2017) Postexercise essential amino acid supplementation amplifies skeletal muscle satellite cell

proliferation in older men 24 hours postexercise. *Physiol. Rep.* 5; e13269.
31. Schiaffino, S. and Bormioli, S. P. (1976) The fate of newly formed satellite cells during compensatory muscle hypertrophy. *Virchows. Arch. B Cell Pathol.* 21; 113–118.
32. Sherr, C. J. (1995) D-type cyclins. *Trends. Biochem. Sci.* 20; 187–190.
33. Smith, C. K., Janney, M. J. and Allen, R. E. (1994) Temporal expression of myogenic regulatory genes during activation, proliferation, and differentiation of rat skeletal muscle satellite cells. *J. Cell Physiol.* 159; 379–385.
34. Steinman, R. A. and Hoffman, B. (1994) Induction of p21 (WAF-1/CIP1) during differentiation. *Oncogene.* 9; 3389–3396.
35. Stockdale, F. E. and Holtzer, H. (1961) DNA synthesis and myogenesis. *Exptl. Cell Res.* 24; 508–520.
36. Tamaki, T., Akatsuka, A., Yoshimura, S., Roy, R. R. and Edgerton, V. R. (2002) New fiber formation in the interstitial spaces of rat skeletal muscle during postnatal growth. *J. Histochem. Cytochem.* 50; 1097–1111.
37. Watkins, S. C. and Cullen, M. J. (1988) A quantitative study of myonuclear and satellite cell nuclear size in Duchenne's muscular dystrophy, polymyositis and normal human skeletal muscle. *Anat. Rec.* 222; 6–11.
38. White, J. D. and Scaffidi, A. (2000) Myotube formation is delayed but not prevented in MyoD-deficient skeletal muscle: studies in regenerating whole muscle grafts of adult mice. *J. Histochem. Cytochem.* 48; 1531–1544.
39. Yablonka-Reuveni, Z. and Rivera, A. J. (1994) Temporal expression of regulatory and structural muscle proteins during myogenesis of satellite cells on isolated adult rat fibers. *Dev. Biol.* 164; 588–603.
40. Zhang, J. M. and Zhao, X. (1999) Direct inhibition of G(1) cdk kinase activity by MyoD promotes myoblast cell cycle withdrawal and terminal differentiation. *EMBO J.* 18; 6983–6993.
41. Zhang, P. and Wong, C. (1999) p21(CIP1) and p57(KIP2) control muscle differentiation at the myogenin step. *Genes. Dev.* 13; 213–224.
42. Zhang, Q., Joshi, S. K., Lovett, D. H., Zhang, B., Bodine, S., Kim, H., *et al.* (2015) Matrix metalloproteinase-2 plays a critical role in overload induced skeletal muscle hypertrophy. *Muscles. Ligaments. Tendons. J.* 4; 446–454.